Nonlinear Combustion Instability in Liquid-Propellant Rocket Motors

Samuel Z. Burstein and Wallace Chinitz

Fourth Quarterly Report

to

Jet Propulsion Laboratory

July 30, 1968

JPL CONTRACT
951946

"This work was performed for the Jet Propulsion Laboratory, California Institute of Technology, as sponsored by the National Aeronautics and Space Administration under Contract NAS7-100."

"This report contains information prepared by Mathematical Applications Group, Inc. (MAGI) under JPL subcontract. Its content is not necessarily endorsed by the Jet Propulsion Laboratory, California Institute of Technology, or the National Aeronautics and Space Administration."

TABLE OF CONTENTS

INTRODUCTION

This report describes the activities of MAGI during the fourth quarter of the contract with the Jet Propulsion Laboratory. During this quarter the effort was directed towards completion of the toroidal motor. In addition, some refinements in the pancake motor have been completed and will be presented. In particular, the ability to represent streakline data graphically is now available as an operator option in the running of program COMB.

The authors would like to acknowledge the strong programming effort of Harold Schechter during the course of this research program.

I. Toroidal Motor - Nonlinear Differential and Difference Equations

The differential equations describing the motion of a compressible fluid in the coordinates θ-Z-t can be given by the vector form

$$\frac{\partial W}{\partial t} + \frac{1}{r}\frac{\partial G}{\partial \theta} + \frac{\partial H}{\partial Z} + H^* \frac{\partial \mathrm{Ln}A}{\partial Z} = \psi \qquad (1)$$

The source term, ψ, has four components corresponding to the rate of production of mass, momentum and energy per unit volume. The vector W also is a four vector, the components of which are the mass, momentum in the θ and Z directions and total energy all per unit volume. The vectors G and H represent the flux of these quantities in the tangential and axial directions respectively. The term containing the logarithmic derivative corresponds to an approximate way of treating small radial variations of the toroidal geometry. It is analogous to the treatment of one-dimensional time dependent flows with an attempt to include area variations. This term can also be considered as a source term of flux proportional to derivative of the logarithmic variation of the area, $A = A(Z)$; the proportionality constant being the flux $H^* = H - p\delta_{i2}$

$$\delta_{i2} = \begin{cases} 1 & \text{for } i = 2 \\ 0 & \text{for } i = 1,3,4 \end{cases}$$

This term allows us to treat, in a simple way, a toroidal subsonic-supersonic nozzle which has an area variation about $r = 1$ (without loss of generality). This will be discussed at greater length in the section on boundary conditions.

The exact form of W is

$$W = \begin{pmatrix} \rho \\ \rho u \\ \rho v \\ \rho(e+\frac{1}{2}(u^2+v^2)) \end{pmatrix} \tag{2}$$

while the components of the tangential flux and axial flux are given as

$$G = \begin{pmatrix} \rho v \\ \rho uv \\ \rho v^2+p \\ (E+p)v \end{pmatrix} \qquad H = \begin{pmatrix} \rho u \\ \rho u^2+p \\ \rho uv \\ (E+p)u \end{pmatrix} \tag{3}$$

The pressure p is a function of the density and specific internal energy through the equation of state

$$p = P(\rho, e) \tag{4}$$

The total energy of the system per unit volume is

$$E = \rho(e+\tfrac{1}{2}(u^2+v^2)).$$

Hence, by using Equation 4 and the above definition of the total energy, this allows one to write the fluxes G = G(W) and H = H(W) only. We may differentiate G and H with respect to W and write Equation 1 in the standard form for quasilinear partial differential equations, i.e.

$$\sum_{i=0}^{n-1} A_i W_{x_i} + B = 0 \tag{5}$$

We associate the matricies **I**, $\partial G/\partial W$ and $\partial H/\partial W$ with A_0, A_1 and A_2 respectively. In this notation our variables become $X_0 = t$, $X_1 = \theta$ and $X_2 = Z$ while the inhomogeneous term is

$$B = H^* \frac{\partial \mathrm{Ln}A}{\partial Z} - \psi \tag{6}$$

Equation 5 will be used as a starting point for the construction of a stable difference approximation of the subsonic inflow condition at the injector face. This will be discussed in the section on boundary conditions.

We seek a solution to Equation 1 by the method of finite difference approximations. Equation 1 is a conservation law. The difference approximation to 1 will also be a conservative difference form; the accuracy of such an approximation will be at least second order. The reader should refer to NASA TR 32-1111 for an example of another application of the following method.

On the periodic space D defined by $t>0$, $0\leq\theta\leq 2\pi$, $0\leq Z\leq L$, we introduce a uniformly spaced mesh or net which consists of the points

$$\theta_i = i\Delta\theta,\ Z_j = j\Delta Z,\ t_n = n\Delta t \qquad i,j,n = 0,1,2,\ldots$$

The set of net points D_h is defined by

$$D_h = \{\theta_i,\ Z_j,\ t_n \mid i=0,1,\ldots;\ j=0,1,\ldots;\ n=0,1,\ldots\}$$

The approximation to $W(\theta_i, Z_j, t_n)$ defined on the space D is given by $V(\theta_i, Z_j, t_n) = V^n_{ij}$ defined on D_h. The approximation that is used is most easily written in two steps.

Let $\tilde{V}^n_{ij}$ be the first predicted value. It is given by

$$\tilde{V}^n_{i+\frac{1}{2},j+\frac{1}{2}} = \frac{1}{4}\left(V^{n-1}_{i+1,j} + V^{n-1}_{i,j+1} + V^{n-1}_{i+1,j} + V_{i,j}\right) \qquad (7a)$$

$$- \frac{\Delta t}{2\Delta\theta}\left[G(V^{n-1}_{i+1,j}) - G\left(V^{n-1}_{i,j}\right) + G(V^{n-1}_{i+1,j+1}) - G(V^{n-1}_{i,j+1})\right]$$

$$- \frac{\Delta t}{2\Delta Z}\left[H(V^{n-1}_{i+1,j+1}) - H(V^{n-1}_{i+1,j}) + H(V^{n-1}_{i,j+1}) - H(V^{n-1}_{i,j})\right]$$

$$- \frac{\Delta t}{4}\left[B(V^{n-1}_{i+1,j}) + B\left(V^{n-1}_{i,j+1}\right) + B\left(V^{n-1}_{i+1,j+1}\right) + B\left(V^{n-1}_{i,j}\right)\right]$$

The final value is obtained from

$$V^n_{i,j} = V^{n-1}_{i,j} - \frac{\Delta t}{4\Delta\theta}\left[G(V^{n-1}_{i+1,j}) - G(V^{n-1}_{i-1,j}) + G(\tilde{V}^n_{i+\frac{1}{2},j+\frac{1}{2}}) - G(\tilde{V}^n_{i-\frac{1}{2},j+\frac{1}{2}}) + G(\tilde{V}^n_{i+\frac{1}{2},j-\frac{1}{2}}) - G(\tilde{V}^n_{i-\frac{1}{2},j-\frac{1}{2}})\right] \qquad (7b)$$

$$- \frac{\Delta t}{4\Delta Z}\left[H(V^{n-1}_{i,j+1}) - H(V^{n-1}_{i,j-1}) + H(\tilde{V}^n_{i+\frac{1}{2},j+\frac{1}{2}}) - H(\tilde{V}^n_{i+\frac{1}{2},j-\frac{1}{2}}) + H(\tilde{V}^n_{i-\frac{1}{2},j+\frac{1}{2}}) - H(\tilde{V}^n_{i-\frac{1}{2},j-\frac{1}{2}})\right]$$

$$- \frac{\Delta t}{2}\left[\frac{1}{4}\left(B(\tilde{V}^n_{i+\frac{1}{2},j-\frac{1}{2}}) + B(\tilde{V}^n_{i+\frac{1}{2},j+\frac{1}{2}}) + B(\tilde{V}^n_{i-\frac{1}{2},j+\frac{1}{2}}) + B(\tilde{V}^n_{i-\frac{1}{2},j-\frac{1}{2}})\right) + B(V^{n-1}_{i,j})\right]$$

The system of equations (7) constitute the difference approximation to Equation 1. One may verify that the System (7) is indeed a second order accurate approximation to Equation 1 by allowing $\delta G = A_1\,\delta V$ and $\delta H = A_2\delta V$. Here δ corresponds to a spatial difference operator in θ or Z and A_1, A_2 are to be taken as constant matrices. Then substituting 7a in 7b and using these definitions for the differences in G and H the result

$$V^n_{i,j} = \dot{V}^{n-1}_{i,j} + \lambda(A_1 + A_2)\,\delta V^{n-1}_{i,j} + \frac{\lambda^2}{2}(A_1 + A_2)^2\delta^2 V^{n-1}_{i,j}$$

$$+ \text{terms } O(\Delta t \cdot B)$$

is obtained. This expression is but the Taylor expansion for V about $t = n\Delta t$ in terms of first and second order space operators δ and δ^2. This shows that the difference approximation is second order accurate.

The periodicity condition in θ on the solution W, i.e.

$$W(\theta,Z,t) = W(\theta+2\pi,Z,t),$$

reduces the problem of finding boundary conditions to just the inflow and outflow conditions at Z = 0 and Z = L. This theory is presented in the next section.

II - Boundary Conditions

A. Injector face (Z = 0)

Only if we were to seek a solution in D where $|Z|<\infty$ (rather than the finite interval $0<Z<L$) would boundary conditions not be required. Such a problem is called an initial value problem. However, since the range of Z is finite, boundary conditions must be prescribed at Z = 0 and Z = L. The natural conditions at the injector, Z = 0, is that the momenta $m = \rho u$ and $n = \rho v$ be prescribed

$$\begin{aligned} m(\theta, 0, t) &= m_o \\ n(\theta, 0, t) &= n_o \end{aligned} \tag{8a}$$

as well as the energy

$$\frac{1}{2}\frac{m_o^2+n_o^2}{\rho_o^2} + e(\theta, 0, t) + p(\theta, 0, t)\rho^{-1}(\theta, 0, t) = L_o \tag{8b}$$

Conditions 8a and 8b are used to simulate the boundary values that one would impose on a gas injected rocket motor. Only axial injection implies $n_o = 0$. Since we are only considering subsonic inflow, one variable cannot be prescribed on the boundary. This is most easily seen by writting Equation 5 in characteristic form. We rewrite Equation 5 as

$$W_t + A_1 W_\theta + A_2 W_Z + B = 0 \tag{9}$$

Let P be a matrix whose eigen vectors are that of A_1. Define V so that W = PV and substitute in Equation 9

$$(PV)_t + A_1(PV)_\theta + A_2(PV)_Z + B = 0 \tag{10}$$

Carrying out the indicated differentiation, there results an equation for V

$$V_t + P^{-1}A_2PV_Z = -P^{-1}\left[B+P_tV+A_2P_ZV+A_1(PV)_\theta\right] \tag{11}$$

which is in the simple characteristic form. We obtained this result by premultiplication by P^{-1}. Now $P^{-1}A\,P = \Lambda$ is diagonal with β_i the elements on the diagonal so that differentiation on the left hand side of Equation 11 is in the characteristic direction

$$\frac{dZ}{dt} = \beta_i \tag{12}$$

i.e., the total differential of V itself is the left member of Equation 11.

The elements β_i are the eigenvalues of A_2; u, u+c and u-c. The direction u-c is left running for u<c; hence this characteristic runs to the boundary Z = 0 from the interior Z>0. The vector V has the components

$$p + v - \rho c^2$$

$$p + \rho cu$$

$$p - \rho cu$$

$$p - v - \rho c^2$$

Hence the data $p - \rho cu$ appears as a total differentiated quantity in the direction u-c; it is given by

$$(p- \rho cu)_t + (u-c)\ (p- \rho cu)_Z = -v(p- \rho cu)_\theta - \rho c^2 v_\theta \tag{13}$$

One simple approximation to Equation 13 is obtained by allowing

$$\overline{\rho c} = \tfrac{1}{2}\left[(\rho c)^{n-1}_{j,0} + (\rho c)^{n-1}_{j,1}\right]$$

$$\bar{v} = \tfrac{1}{2}\left[v^{n-1}_{j,0} + v^{n-1}_{j,1}\right]$$

$$\bar{u} = \tfrac{1}{2}\left[u^{n-1}_{j,0} + u^{n-1}_{j,1}\right]$$

then solving for the pressure by using forward differences for the time and Z space differences (θ differences can be centered)

$$P^{n}_{j,0} = P^{n-1}_{j,0} + \overline{\rho c}\,(u^{n}_{j,1}-u^{n-1}_{j,1}) + \frac{\Delta t}{\Delta Z}(\bar{u}-\bar{c})\left[p^{n-1}_{j,0}-p^{n-1}_{j,1} - \overline{\rho c}\,(u^{n-1}_{j,0}-u^{n-1}_{j,1})\right] - \bar{v}\,\frac{\Delta t}{4\Delta\theta}\left[p^{n-1}_{j+1,0}-p^{n-1}_{j-1,0}+p^{n}_{j+1,1}-p^{n}_{j-1,1}\right]$$

$$+ \overline{\rho c}\,\bar{v}\,\frac{\Delta t}{4\Delta\theta}\left[u^{n-1}_{j+1,0}-u^{n-1}_{j-1,0}+u^{n}_{j+1,1}-u^{n}_{j-1,1}\right] - \overline{\rho c}^{2}\,\frac{\Delta t}{4\Delta\theta}\left[v^{n}_{j+1,1}-v^{n}_{j-1,1}\right] \qquad (14)$$

Now that the pressure is known at the advanced time $n\Delta t$ on the injector face, $Z = j\Delta Z = 0$, we solve for the density ρ from Equations 8a, 8 b and 4. The following result is obtained from the positive root of the quadratic equation in the density,

$$\rho = \frac{\gamma p}{2(\gamma-1)L_o}\left\{1 + \left[1+2L_o\left(\frac{(\gamma-1)m_o}{\gamma p}\right)\right]^{\frac{1}{2}}\right\} \qquad (15)$$

An iterative procedure could now be used by redefining the barred quantities $\bar{\rho}$ and $\bar{c}$ in terms of the latest estimate of the density, which is given above. The present status of the toroidal motor code does not do this, however it is to be included in a future version. Now that the density is known, as well as the pressure, all the data required to advance the solution to the next time

level is known. The next section considers the boundary condition at the plane of outflow, Z = L.

B. Nozzle exit plane (Z = L)

The simplest and perhaps best way of treating an outflow condition is to impose the same condition on all the characteristics: that they have positive slope (all $\beta_i > 0$) when the flow velocity is $u > 0$. This means that if at the boundary Z = L, the flow is supersonic, then all three characteristics with slope u, $u \pm c$ will intersect the exit plane when originating from the interior of D. Then the boundary is completely specified by the interior flow field conditions. Conversely, information specified at the boundary because of the geometry of the characteristics can have an effect only on the field to the right, or outside of D.

We impose this condition at the boundary by specifying a schedule of area variation in the axial direction, $\delta \mathrm{Ln}A/\delta Z$. At some arbitrary point, say $Z = \ell$ the chamber length, the area decreases simulating a converging nozzle section. At a section further downstream, $\ell < Z_t < L$ the area then increases up to the point Z = L. The throat of our motor corresponds to Z_t and the diverging section, of length $L-Z_t$, produces a sufficiently strong supersonic outflow condition. The only conditions imposed on how one choses such an area variation is the restriction on an allowable flow rate for the steady state of the rocket motor. Hence, the ratio of the chamber area $A(Z<\ell)$ to the throat area $A(Z_t)$ is determined by allowing the Mach number at the throat section to be unity for the desired rate of flow specified at the injector. The area at

the exit plane of the motor, $A(Z = L)$, is chosen to produce a Mach number of the flow sufficiently greater than one so that even under transient conditions the outflow will remain supersonic.

Then the boundary condition specified at $Z = L$ is

$$W(\theta, L, t) = W(\theta, L-\Delta Z, t).$$

This corresponds to zero order extrapolation and is sufficient to produce smooth results. This completes the discussion of the boundary conditions. The next section presents some results of a calculation using these boundary conditions in the toroidal motor.

III - Results of a Test Case

The previously described theory was coded and a test case was generated for the program. We wanted to see the convergence of the calculation to a solution from somewhat arbitrary initial data. The initial data prescribed is

$$\left.\begin{aligned} p &= 1. \\ \rho &= 1. \\ u/\sqrt{\gamma} &= 0.4 \\ v &= 0 \end{aligned}\right\} \quad 0 \le Z \le \ell$$

$$\left.\begin{aligned} p &= p(Z) \\ \rho &= \rho(Z) \\ u &= u(Z) \\ v &= 0 \end{aligned}\right\} \quad \ell < Z \le L$$

The exit Mach number was approximately two for the area variation chosen. The exact dependence of the density pressure and velocity was linear in Z, the endpoint values p(L), ρ(L) and u(L) being obtained from one-dimensional reversible flow tables at γ = 1.2. Table one below shows the convergence of the solution at the exit plane of the combustor.

Table 1 - Toroidal Motor Convergence

Pressure	Iteration cycle Number
1.0	0
0.57281	200
0.52067	400
0.51894	600
0.52048	800
0.52018	1000

Figures 1, 2, and 3 are CalComp plots of the density ρ, pressure p, and velocity $(u^2+v^2)^{\frac{1}{2}}$. In this test case v = 0 for all time so that the calculation is essentially one-dimensional as Figure 3 shows. In Figures 1 and 2 one observes a gradient in the density and pressure at the injector face. This gradient occurs through the low order accuracy of the treatment of the boundary condition at the injector face. As was stated in the previous section, an iterative procedure will be employed that will reduce the truncation error of the boundary calculation so as to improve on this inaccuracy.

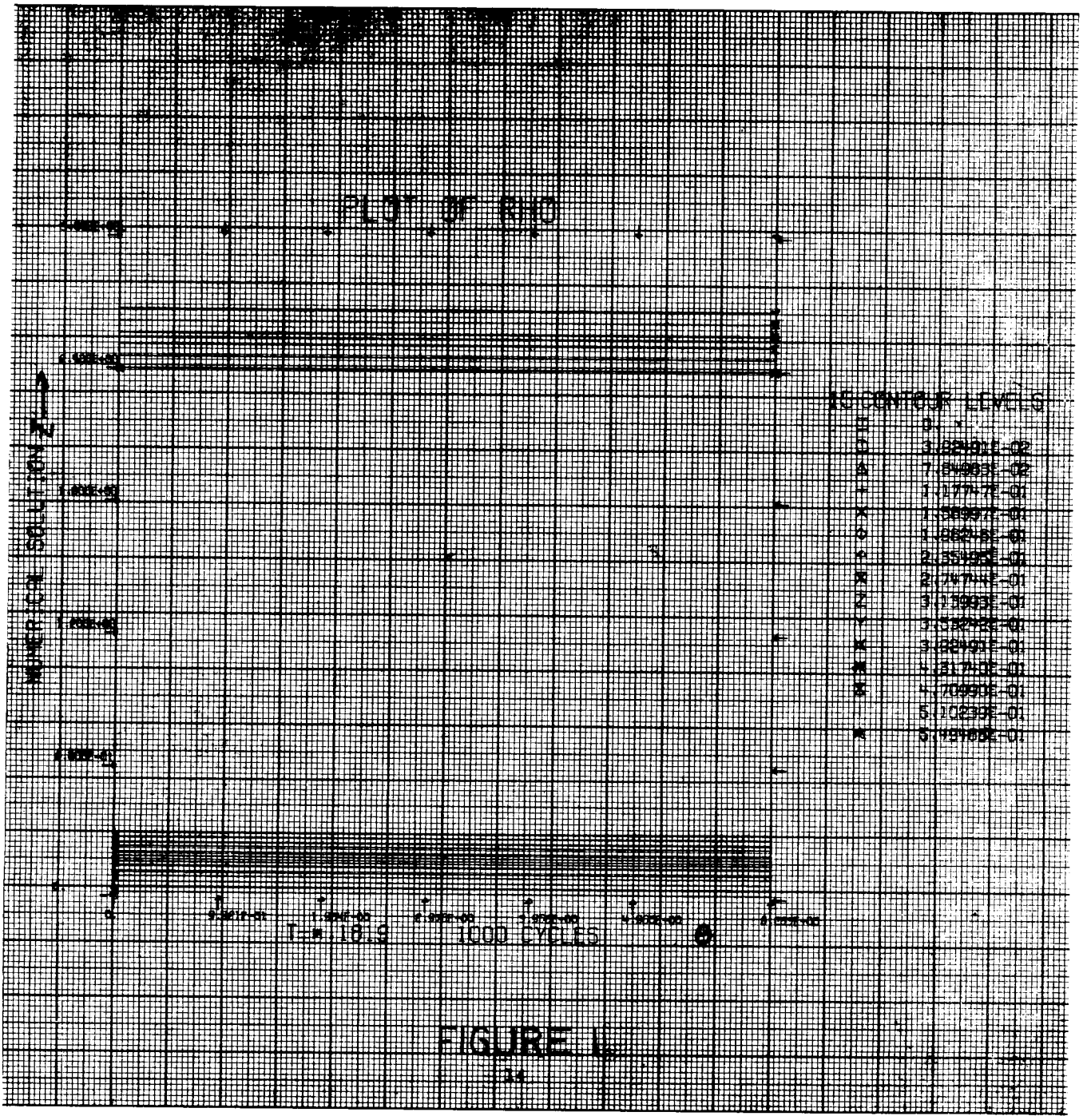

FIGURE 1.

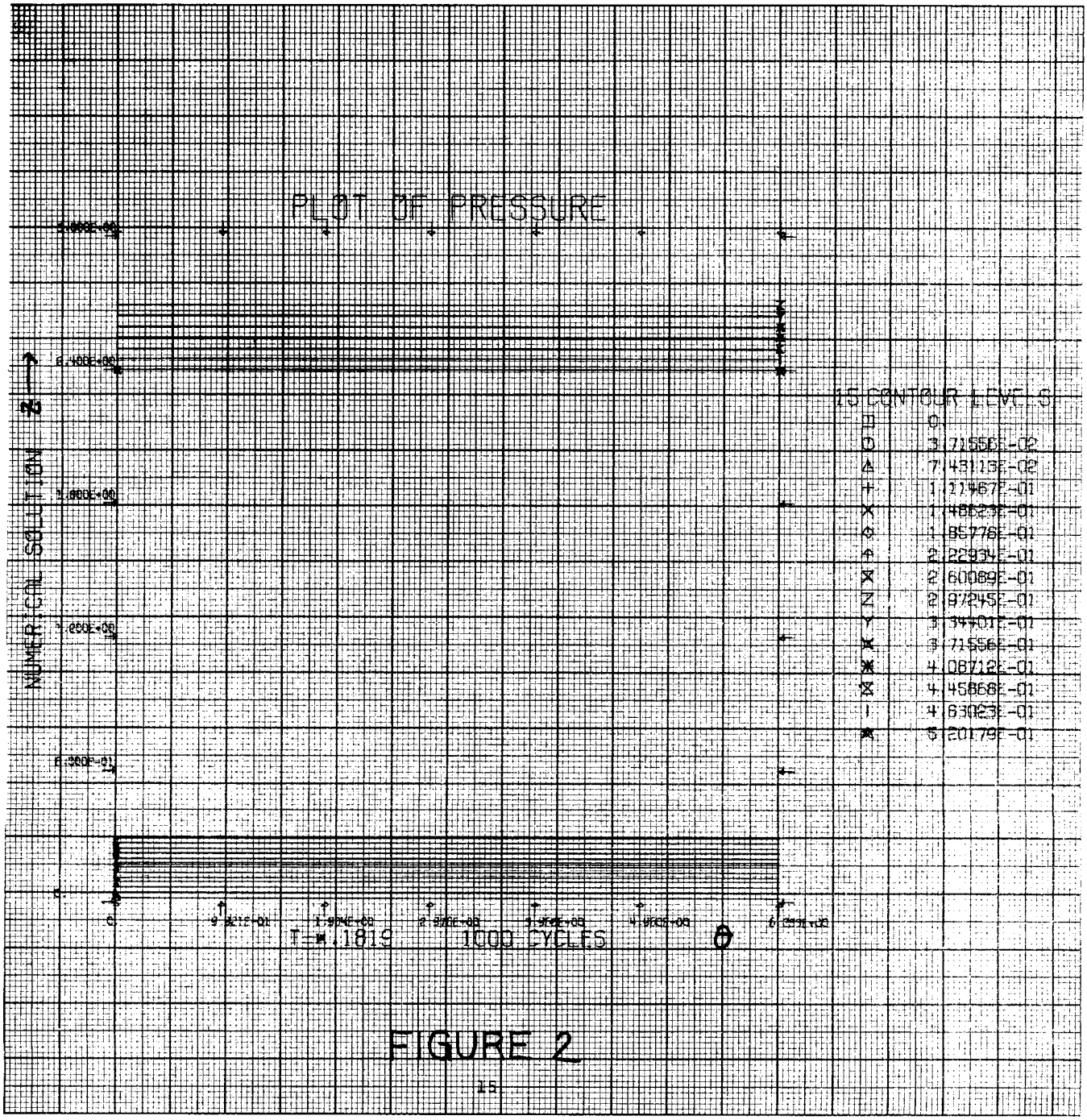
PLOT OF PRESSURE
15 CONTOUR LEVELS
0.
3.71556E-02
7.43113E-02
1.11467E-01
1.48623E-01
1.85778E-01
2.22934E-01
2.60089E-01
2.97245E-01
3.34401E-01
3.71556E-01
4.08712E-01
4.45868E-01
4.83023E-01
5.20179E-01
T=4.1819
1000 CYCLES

FIGURE 2

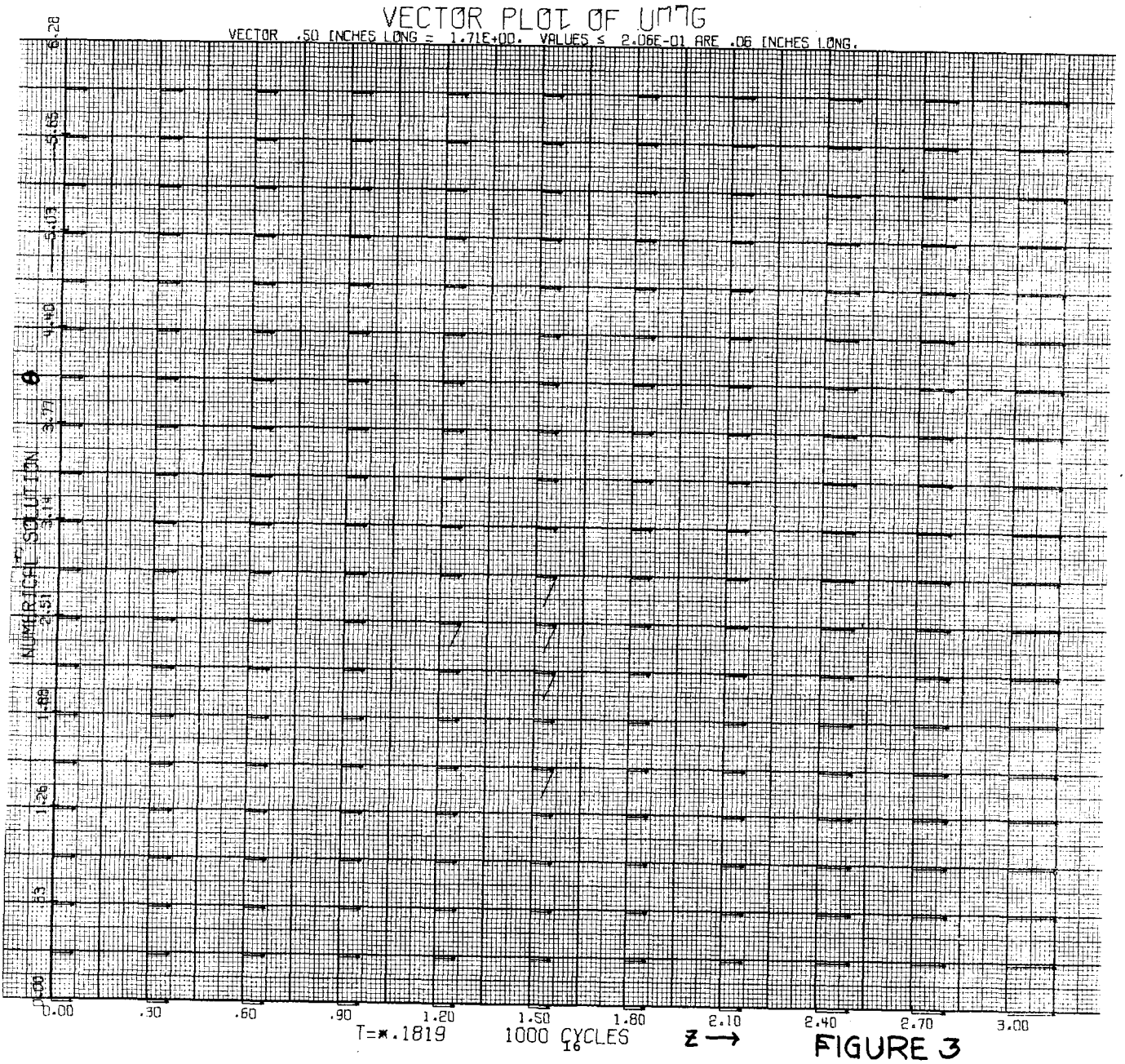
VECTOR PLOT OF UMG
VECTOR .50 INCHES LONG = 1.71E+00. VALUES ≤ 2.06E-01 ARE .06 INCHES LONG.
6.28
5.65
5.03
4.40
3.77
3.14
2.51
1.88
1.26
.63
.00
NUMERICAL SOLUTION
0.00
.30
.60
.90
1.20
1.50
1.80
2.10
2.40
2.70
3.00
T=*.1819
1000 CYCLES
16
Z →

FIGURE 3

IV - Program COMB Status

In this section we present some recent results of a test run using the pancake motor computer program. As was stated on page 55 in the third quarterly report to the Jet Propulsion Laboratory, work was progressing on the ability of program COMB to produce instantaneous streakline pictures of particles moving in the r-θ plane. This feature is now included in the computer program; a test case has been completed and the results are presented in Figures 4 through 15.

Figures 1, 2 and 3 correspond to the initial data for this calculation, the density, the pressure and the velocity respectively. For this case the max (min) pressure is 590 psia (10 psia). Figure 7 is the velocity field after almost one cycle of rotation of the pressure wave. Figure 8 is a plot of a streakline obtained by integrating the motion of a point (starting at the midpoint of the first quadrant, $\theta=\pi/4$, r=0.5) over the first 500 cycles of calculation. The point ends near its starting position moving in a clockwise fashion which is the same direction as the wave. Linear theory would have the point moving in closed elliptical paths. Figure 9 completes the motion of the particle through 1000 cycles of calculation. Here, in Figure 9, the fluid motion can be considered to be 'steady'; at least the nonlinear aspects of the motion are well defined. The particle stays within the first quadrant of the motor.

Figure 7 shows the particle motion with the starting transient included. The velocity field at the instant t = 6.7596 is shown in Figure 10.

Figure 11 is the nondimensional pressure field at 500 cycles and the dimensional pressure on the circumference of the motor at this same time is shown in Figure 12. Figures 13 and 14 also show the same corresponding quantities as Figures 11 and 12 but at 1000 cycles, when the wave has completed almost two and one-half rotations. Finally, Figure 15 shows the density field at 1000 cycles. The program is flexible in that it can print out any or every one of these graphed quantities at prescribed intervals of time. The intervals and selection of graph combinations are under operator control via input data cards.

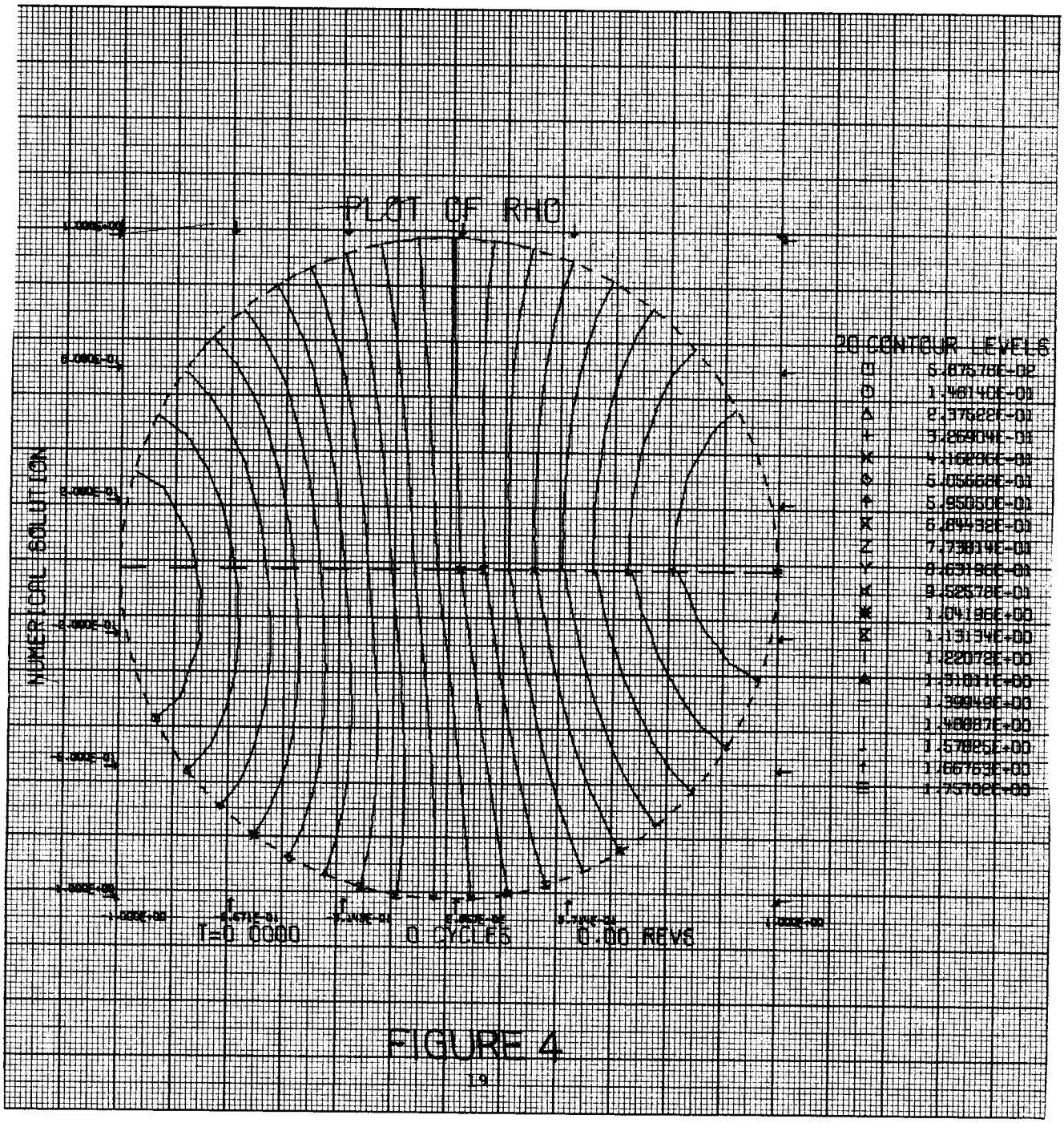
PLOT OF RHO
20 CONTOUR LEVELS
5.875780E-02
1.461405E-01
2.376222E-01
3.269904E-01
4.168286E-01
5.056668E-01
5.950500E-01
6.844332E-01
7.738014E-01
8.631966E-01
9.525780E-01
1.041966E+00
1.131346E+00
1.220728E+00
1.310111E+00
1.399493E+00
1.488887E+00
1.578269E+00
1.667652E+00
1.757034E+00
T=0.0000
0 CYCLES
0.00 REVS

FIGURE 4

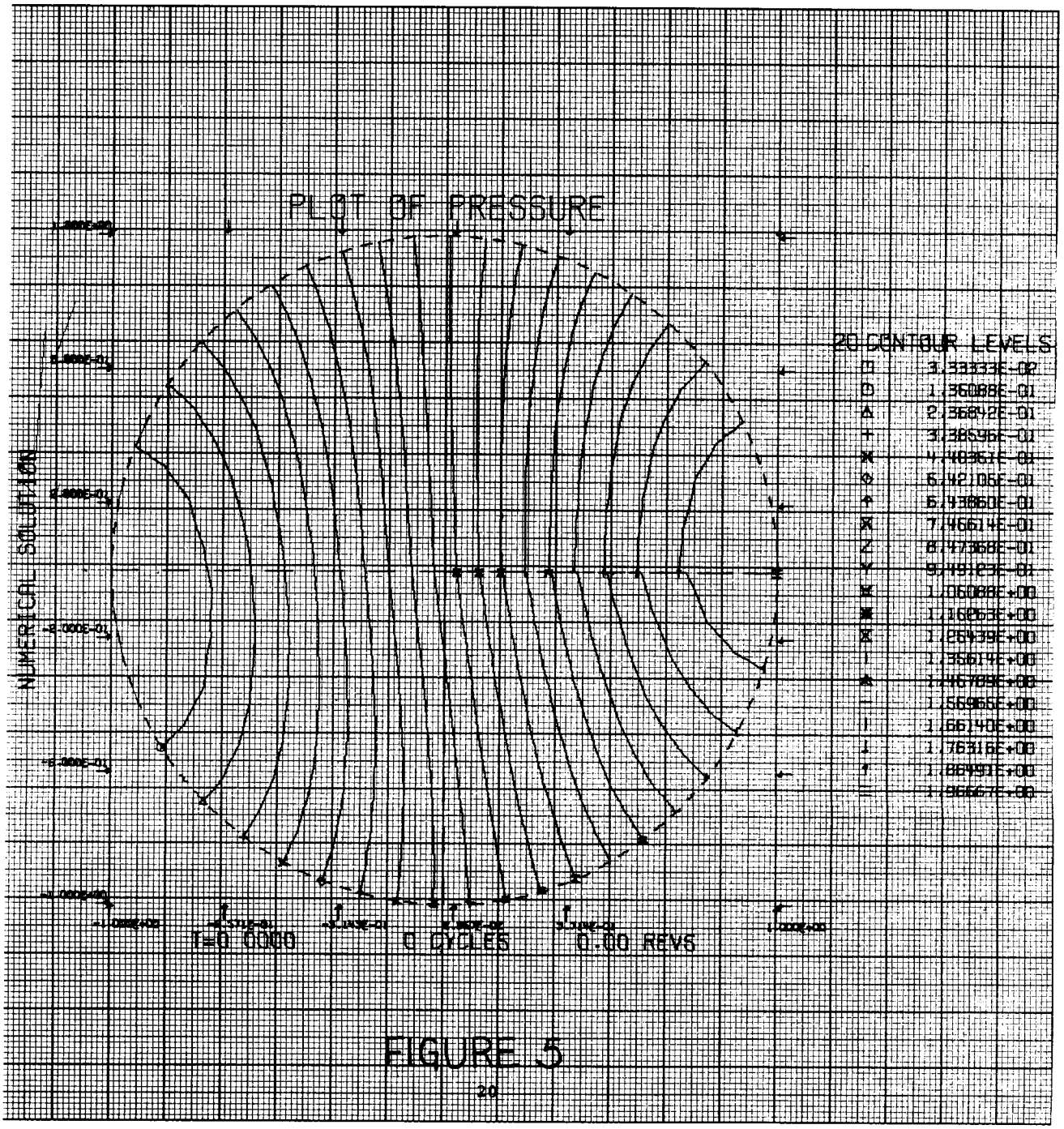
PLOT OF PRESSURE
NUMERICAL SOLUTION
20 CONTOUR LEVELS
3.333333E-02
1.360088E-01
2.386842E-01
3.413596E-01
4.440351E-01
5.467105E-01
6.493860E-01
7.520614E-01
8.547368E-01
9.574123E-01
1.060088E+00
1.162763E+00
1.265439E+00
1.368114E+00
1.470789E+00
1.573465E+00
1.676140E+00
1.778816E+00
1.881491E+00
1.984167E+00
T=0.0000
0 CYCLES
0.00 REVS

FIGURE 5

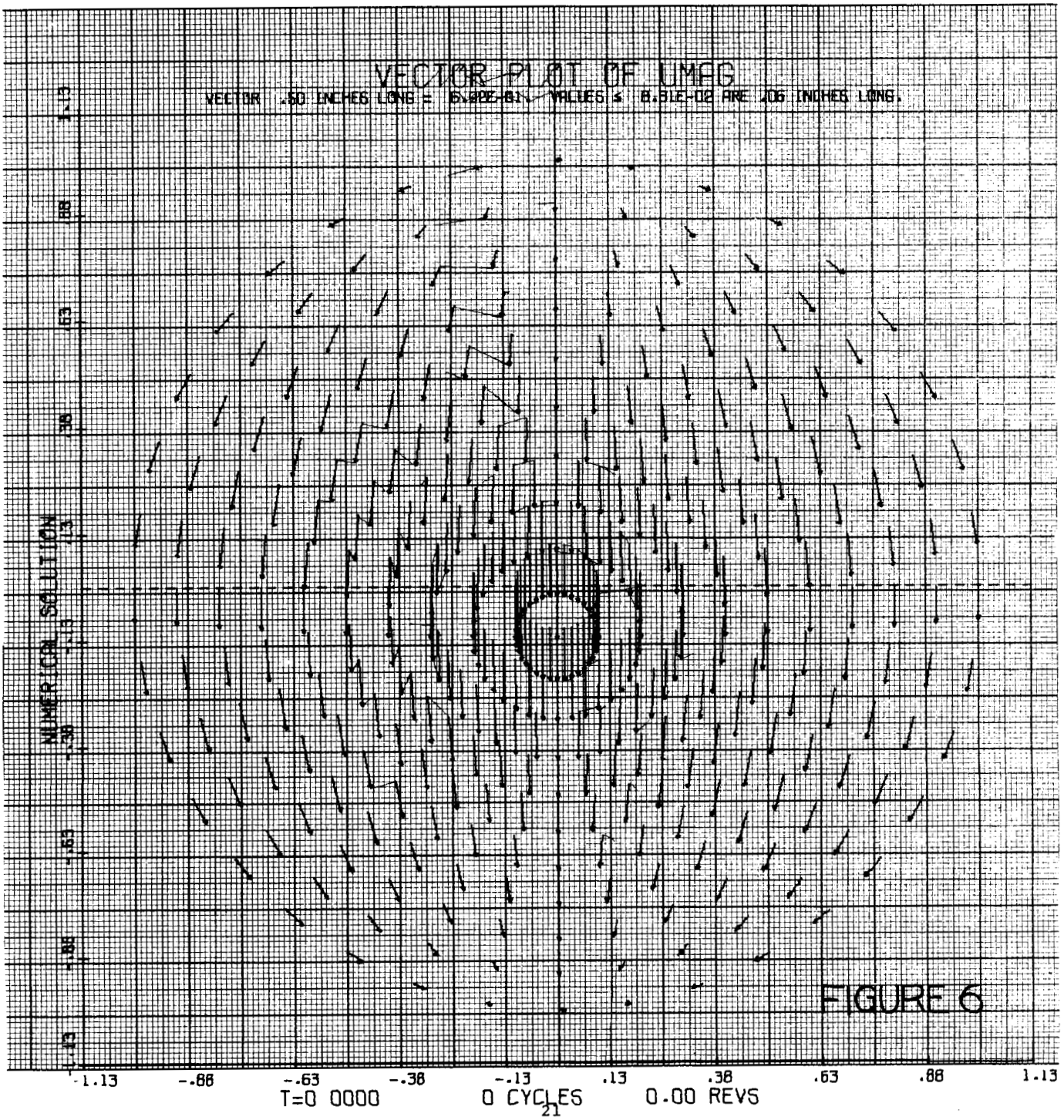
VECTOR PLOT OF UMEG
VECTOR .50 INCHES LONG = 6.20E-01. VALUES ≤ 8.51E-02 ARE .06 INCHES LONG.
NUMERICAL SOLUTION
1.13
.88
.63
.38
.13
-.13
-.38
-.63
-.88
-1.13
-1.13
-.88
-.63
-.38
-.13
.13
.38
.63
.88
1.13
T=0 0000
0 CYCLES
0.00 REVS

FIGURE 6

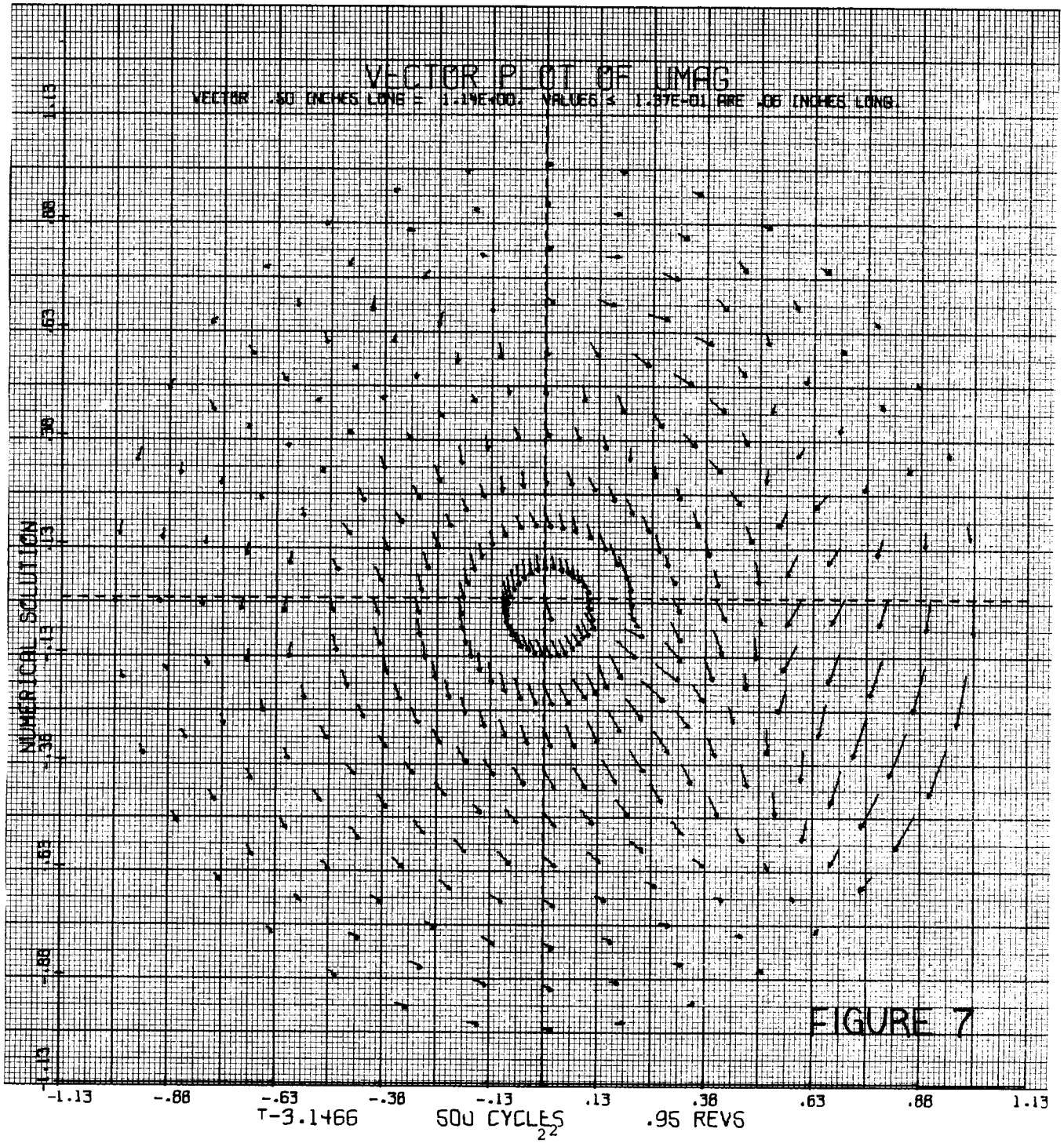
VECTOR PLOT OF UMAG
VECTOR .50 INCHES LONG = 1.14E+00. VALUES ≤ 1.37E-01 ARE .06 INCHES LONG.
NUMERICAL SOLUTION
1.13
.88
.63
.38
.13
-.13
-.38
-.63
-.88
-1.13
-1.13
-.88
-.63
-.38
-.13
.13
.38
.63
.88
1.13
T-3.1466
500 CYCLES
.95 REVS

FIGURE 7

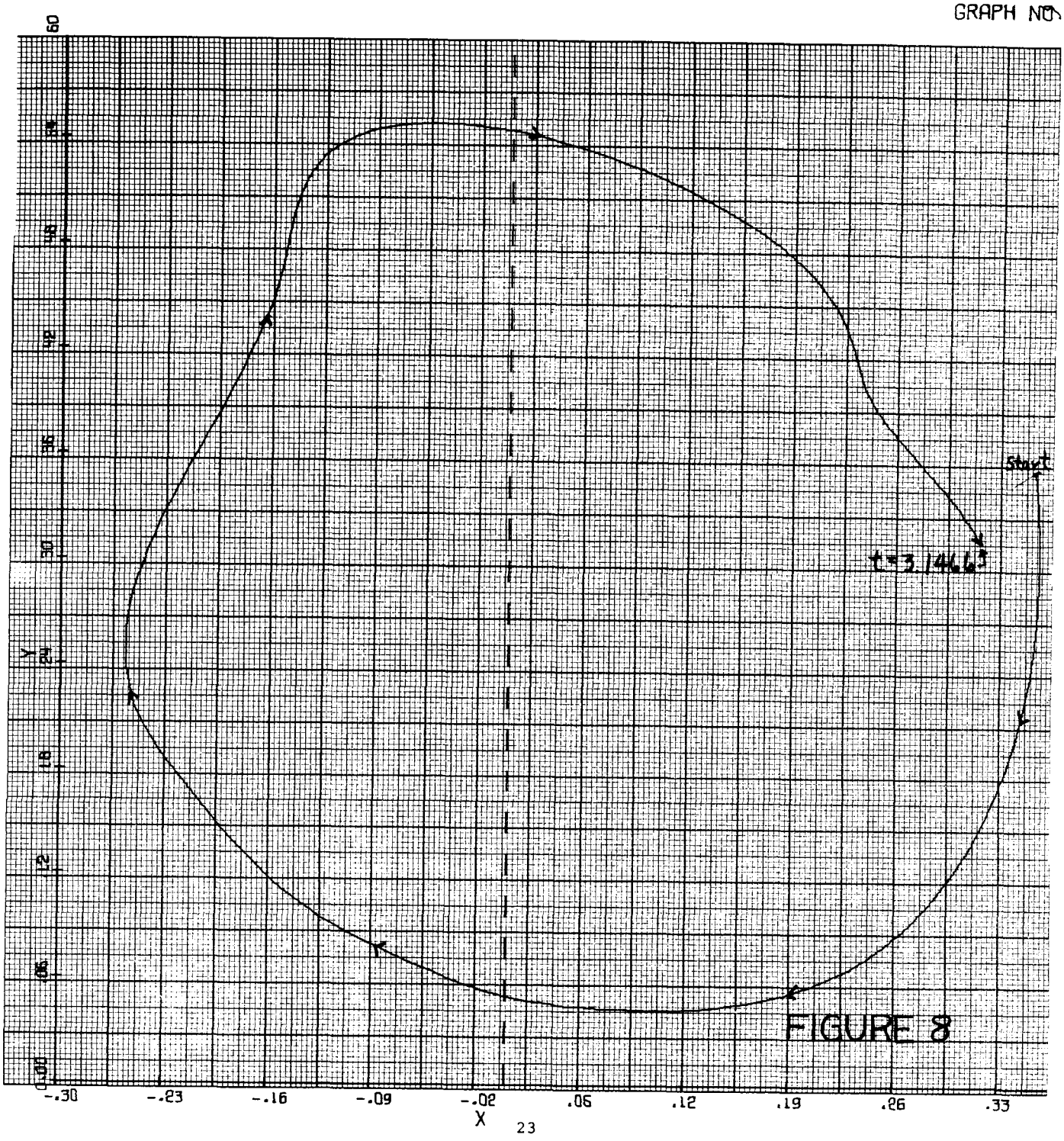
GRAPH NO.
.60
.48
.36
.24
.12
0
-.12
-.24
-.36
-.48
-.60
Y
-.30
-.23
-.16
-.09
-.02
.06
.12
.19
.26
.33
X
Start
t=3.1466

FIGURE 8

GRAPH NO.

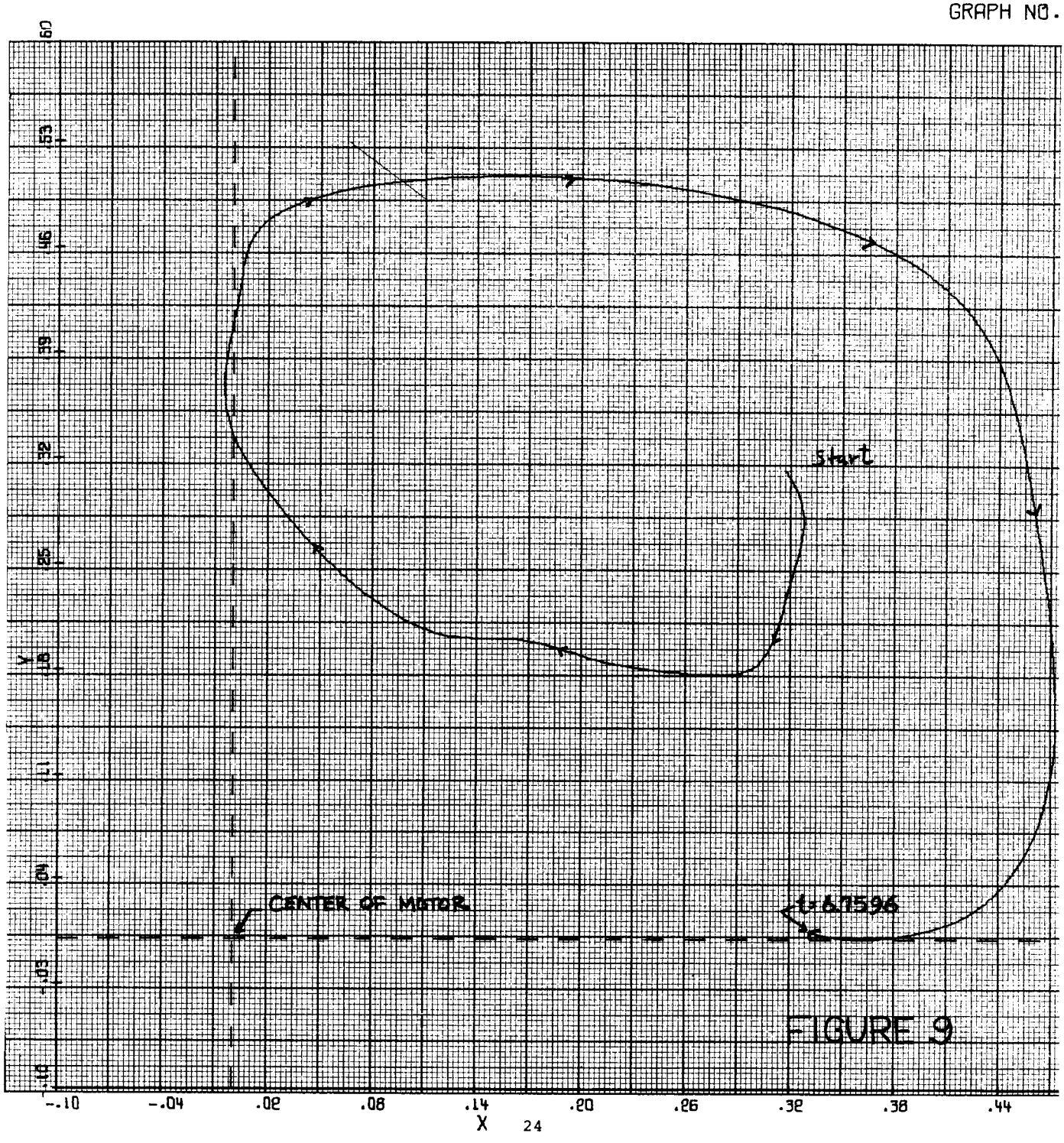

FIGURE 9

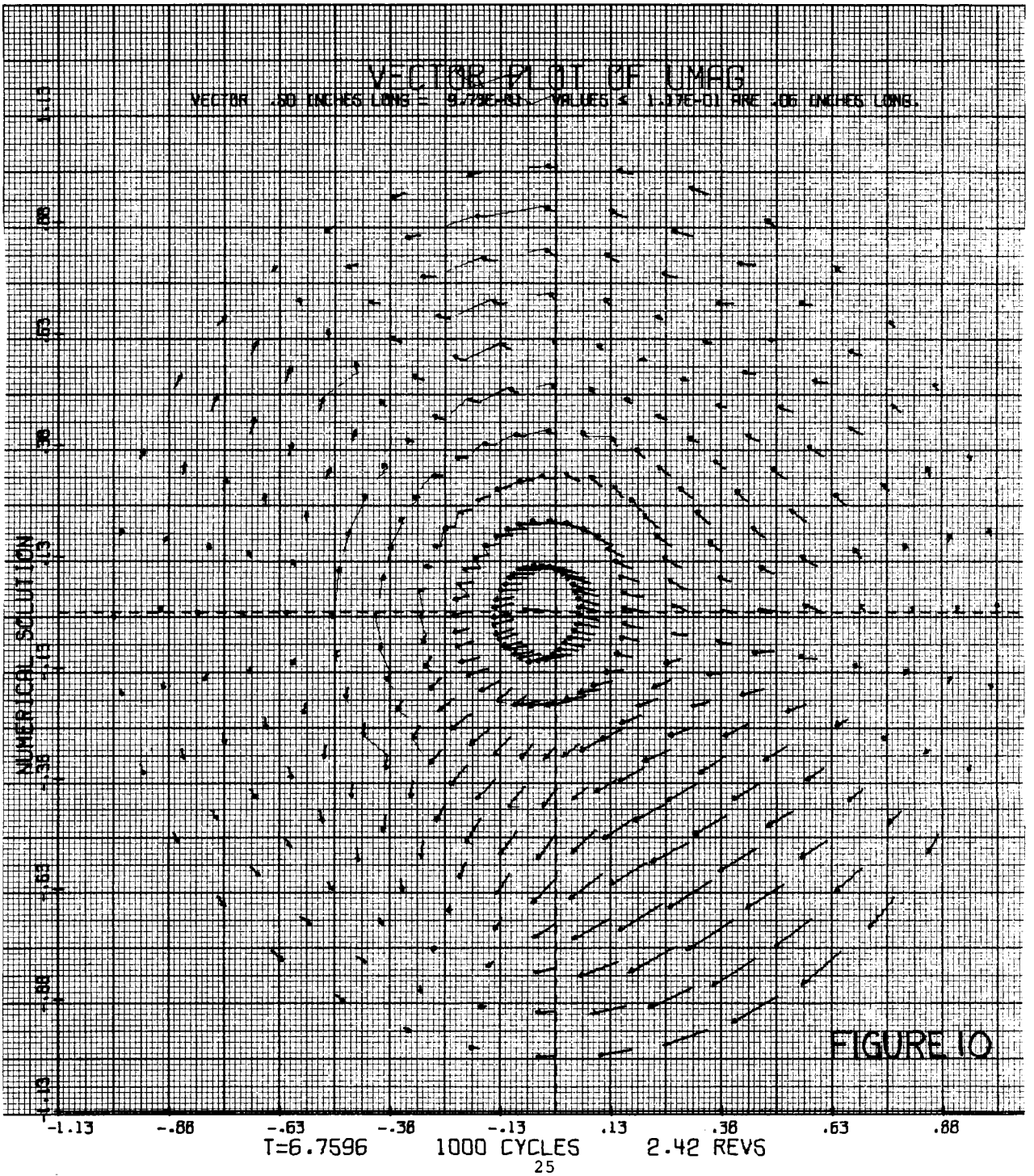
VECTOR PLOT OF UMAG
VECTOR .80 INCHES LONG = 9.77E-03. VALUES < 1.17E-01 ARE .06 INCHES LONG.
NUMERICAL SOLUTION
1.13
.88
.63
.38
.13
-.13
-.38
-.63
-.88
-1.13
-1.13
-.88
-.63
-.38
-.13
.13
.38
.63
.88
T=6.7596 1000 CYCLES 2.42 REVS

FIGURE 10

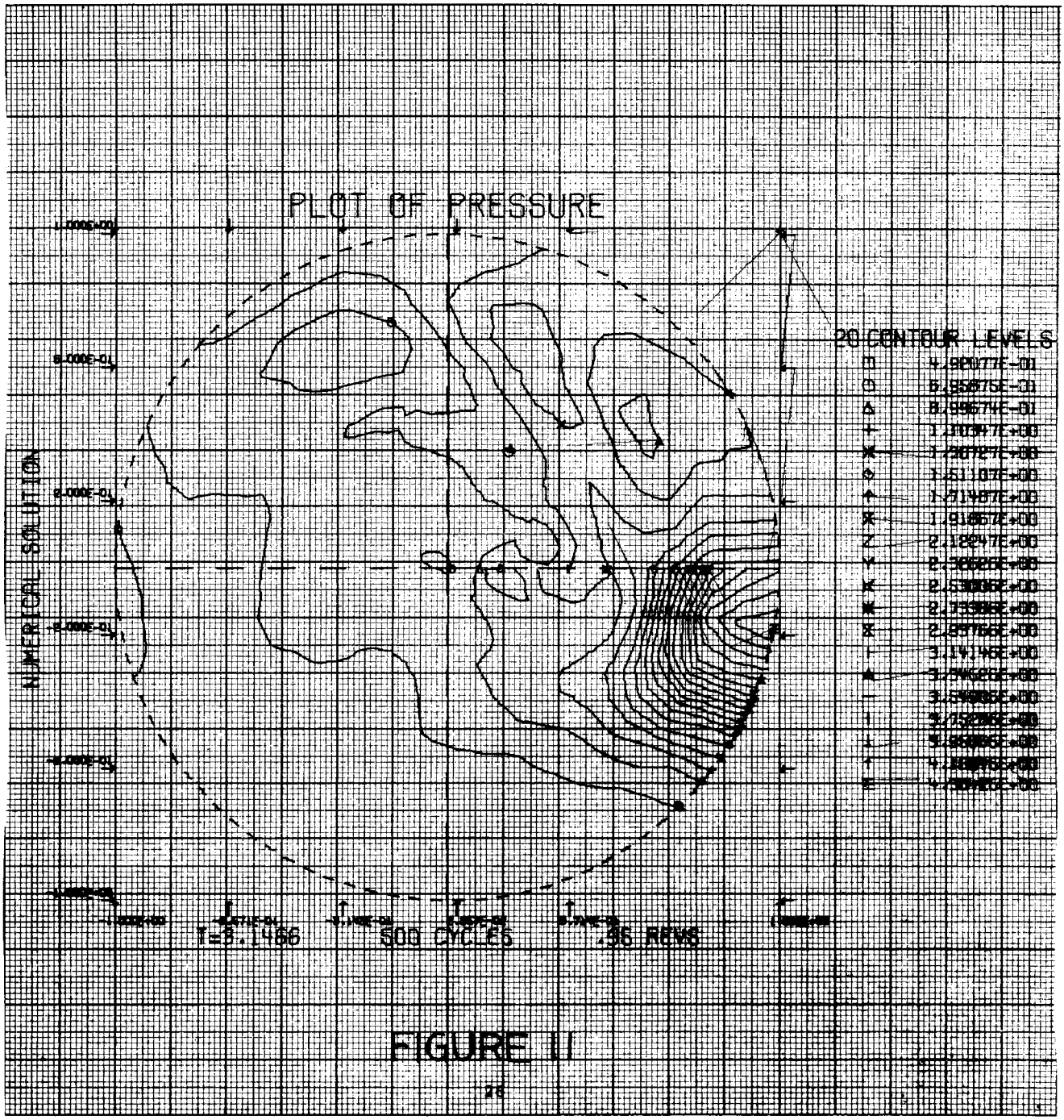
PLOT OF PRESSURE
NUMERICAL SOLUTION
20 CONTOUR LEVELS
T=3.1466
500 CYCLES
.36 REVS

FIGURE 11

GRAPH NO. 2

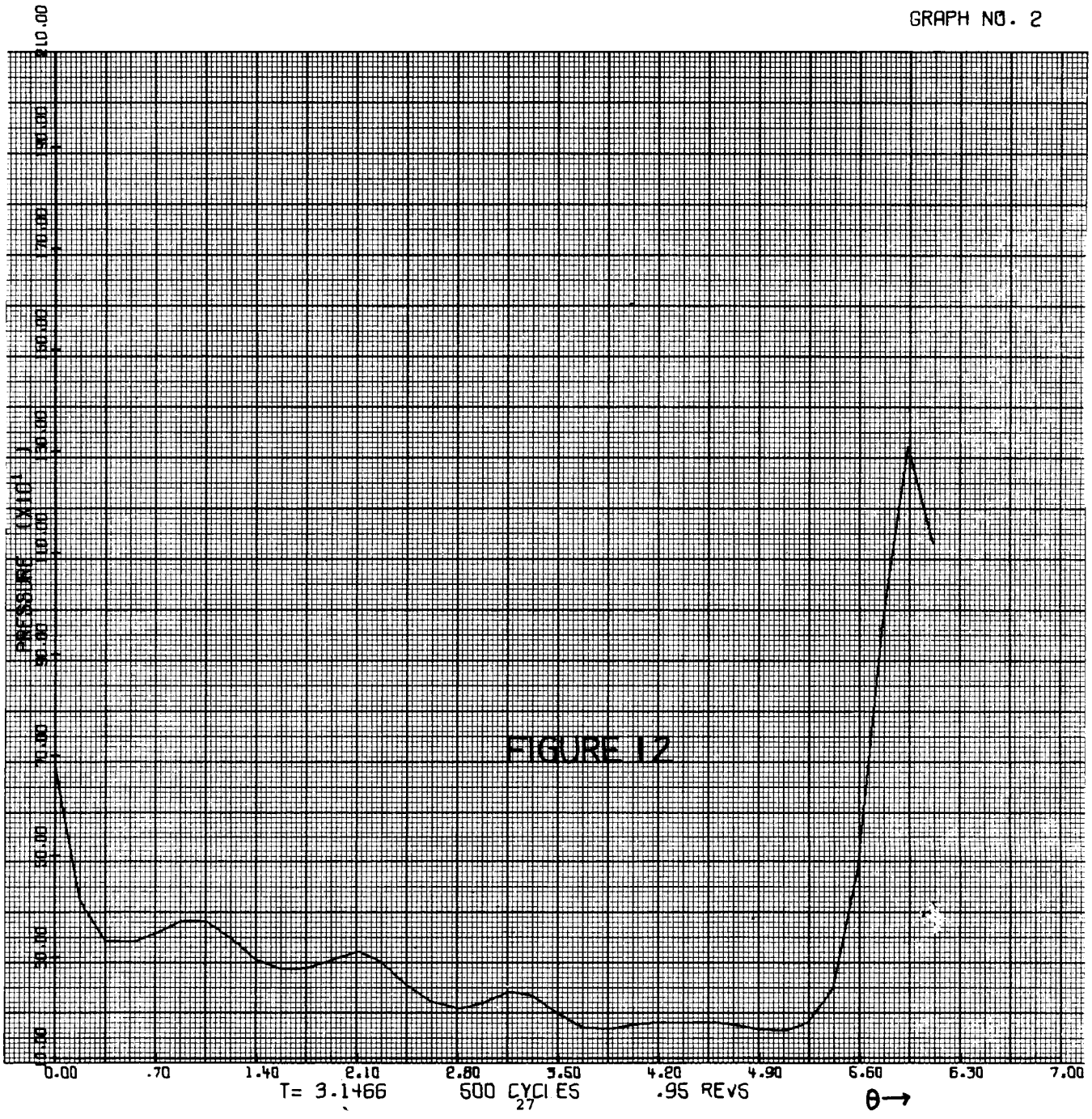

FIGURE 12

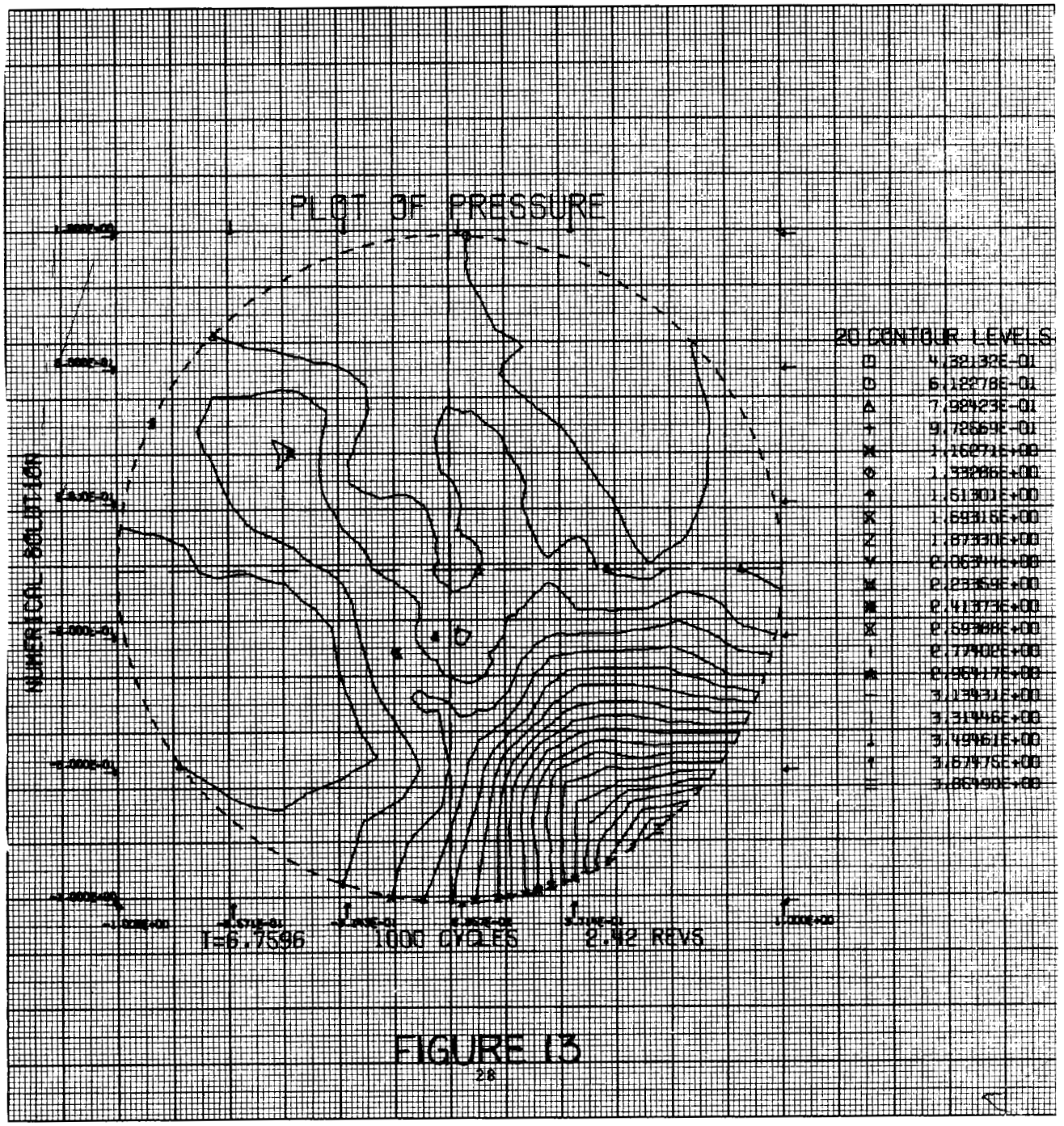
PLOT OF PRESSURE
20 CONTOUR LEVELS
T=6.7596
1000 CYCLES
2.42 REVS

FIGURE 13

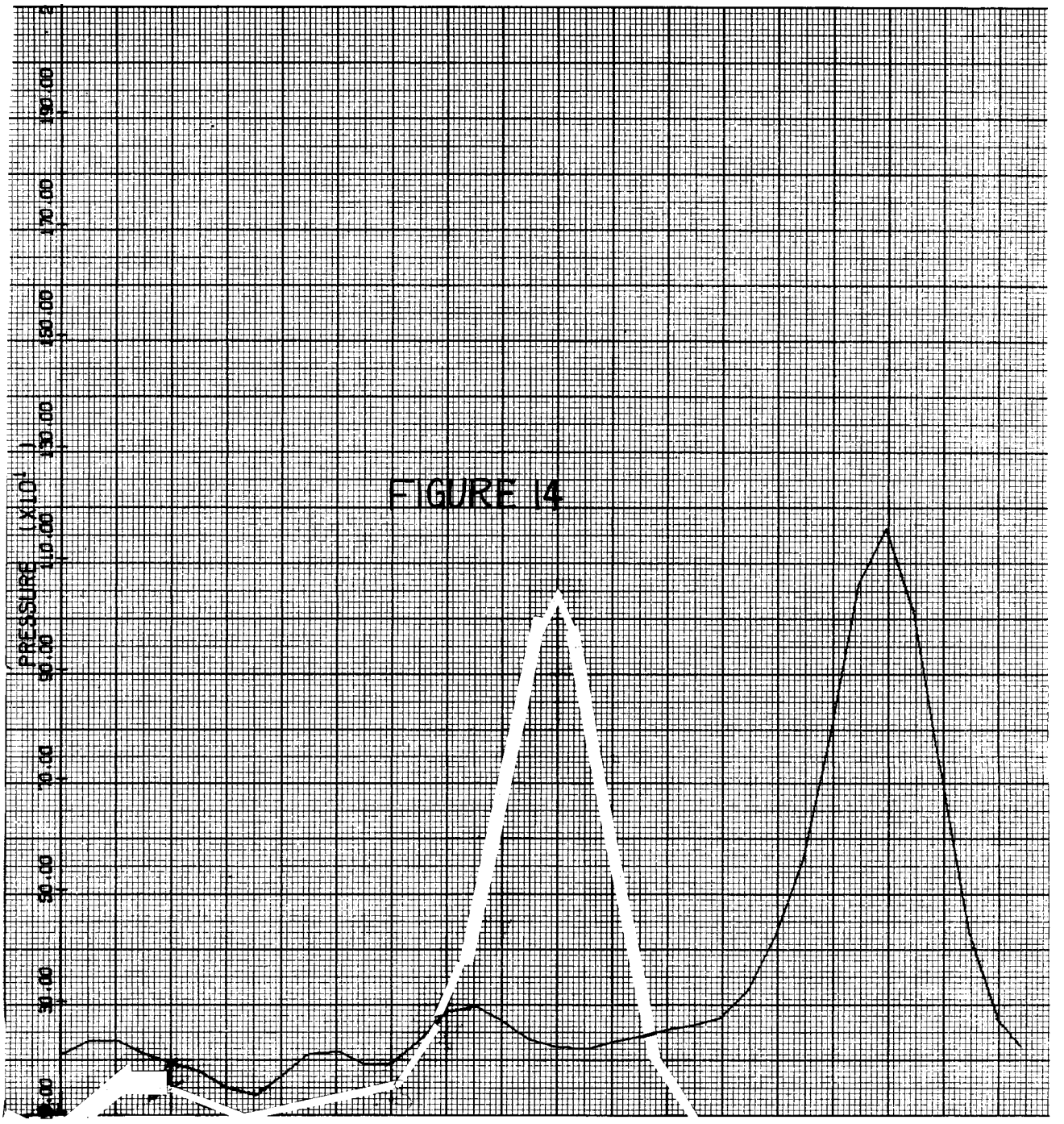
PRESSURE (X10³)
200.00
170.00
150.00
130.00
110.00
90.00
70.00
50.00
30.00
10.00

FIGURE 14

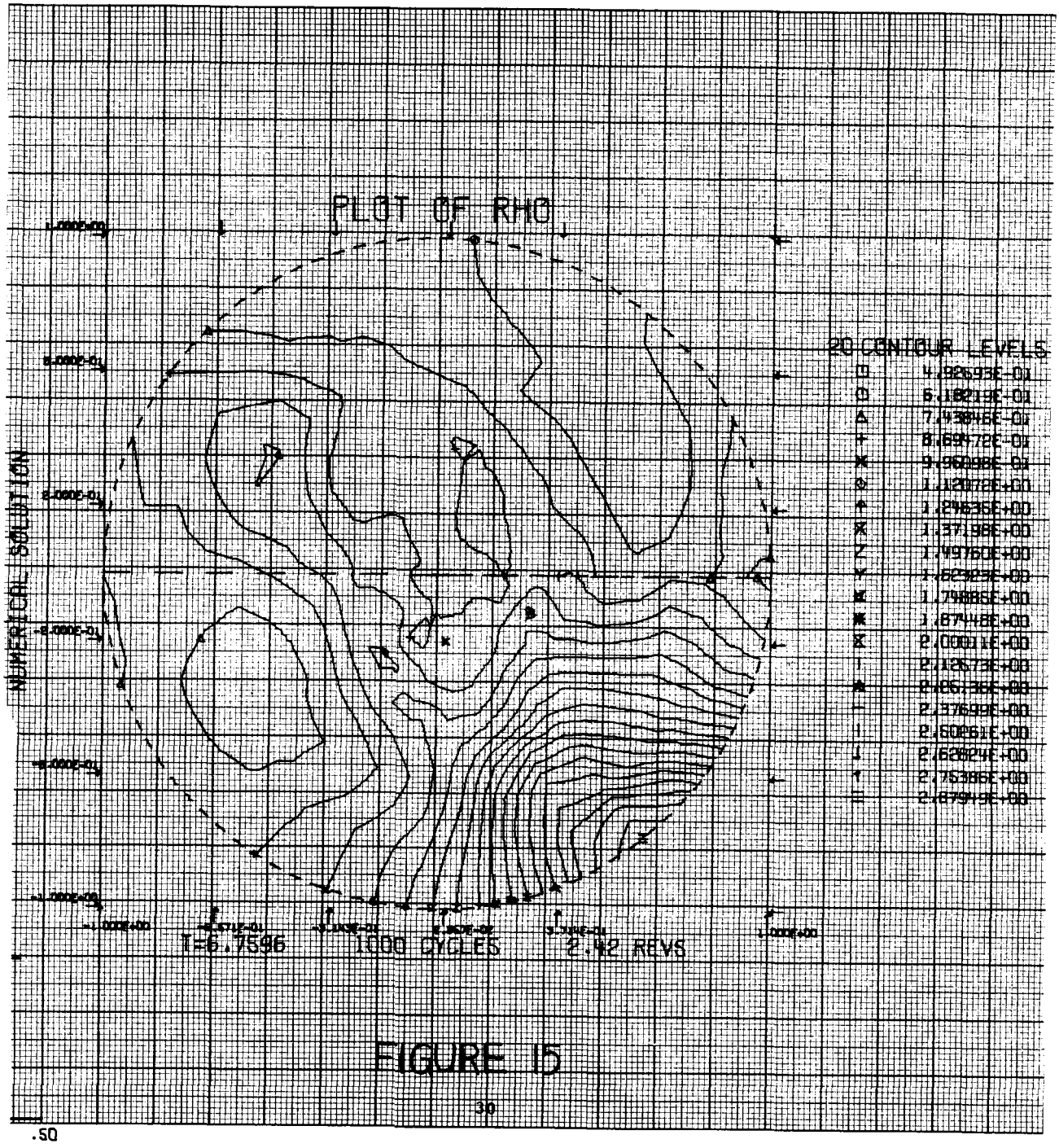
PLOT OF RHO
NUMERICAL SOLUTION
20 CONTOUR LEVELS
T=6.7596
1000 CYCLES
2.42 REVS
.50

FIGURE 15